

International Journal of Modern Physics E
© World Scientific Publishing Company

A bag model of matter condensed by the strong interaction

Zhi-Qiang Miao

Department of Astronomy, Xiamen University, Xiamen, Fujian 361005, China

Cheng-Jun Xia

Center for Gravitation and Cosmology, College of Physical Science and Technology, Yangzhou University, Yangzhou 225009, China

*School of Information Science and Engineering, NingboTech University, Ningbo 315100, China
Advanced Science Research Center, Japan Atomic Energy Agency, Shirakata 2-4, Tokai, Ibaraki 319-1195, Japan
cjxia@yzu.edu.cn*

Xiao-Yu Lai

Department of Physics and Astronomy, Hubei University of Education, Wuhan 430205, China

Toshiki Maruyama

Advanced Science Research Center, Japan Atomic Energy Agency, Shirakata 2-4, Tokai, Ibaraki 319-1195, Japan

Ren-Xin Xu

*School of Physics and State Key Laboratory of Nuclear Physics and Technology, Peking University, Beijing 100871, China
Kavli Institute for Astronomy and Astrophysics, Peking University, Beijing 100871, China
r.x.xu@pku.edu.cn*

En-Ping Zhou

School of Physics, Huazhong University of Science and Technology, 1037 Luoyu Road, Wuhan, 430074, China

Received 18 11 2021

Inspired by various astrophysical phenomenons, it is suggested that pulsar-like compact stars are comprised entirely of strangeons (quark-clusters with three-light-flavor symmetry) and a small amount of electrons. In order to better constrain the properties of strangeon stars, we propose a linked bag model to describe the condensed matter by the strong interaction (i.e., strong condensed matter) in both 2-flavoured (nucleons) and 3-flavoured (hyperons, strangeons, etc.) scenarios. The model parameters are calibrated to reproduce the saturation properties of nuclear matter, which are later applied to hyperon matter and strangeon matter. Compared with baryon matter, the derived energy per baryon of strangeon matter is reduced if the strangeon carries a large number of valence quarks, which stiffens the equation of state and consequently increases the maximum mass of strangeon stars. In a large parameter space, the maximum mass and tidal deformability of strangeon stars predicted by the linked bag model are consistent with

2 *Miao, Xia, Lai, Maruyama, Xu, and Zhou*

the current astrophysical constraints. It is found that the maximum mass of strangeon stars can be as large as $\sim 2.5M_\odot$, while the tidal deformability of a $1.4M_\odot$ strangeon star lies in the range of $180 \lesssim \Lambda_{1.4} \lesssim 340$.

Keywords: bag model; compact stars.

PACS numbers: 21.30.Fe, 26.60.+c, 21.65.+f

1. Introduction

What is the state of matter if normal baryon matter is compressed so tightly that baryons come into close contact? This question is not only relevant to low-energy strong force, as in the case of nuclear physics, but also important to unveil an interesting piece of Nature: the huge and dense lump created in a core-collapse supernova. The density of matter in the lump is extremely high, which may even surpass $5n_0$ in the center region with n_0 being the nuclear saturation density. Two questions are frequently raised in the study of such core-compressed matter:¹ 1. Does deconfinement phase transition take place^{2–13}? 2. Does strangeness play an important role^{14–27}?

Since it is still challenging to simulate dense matter with lattice QCD, to answer those questions, we need to rely on various constraints from both nuclear and astrophysical studies. So far, the properties of nuclear matter around the saturation density ($n_0 \approx 0.16 \text{ fm}^{-3}$) are well constrained with the binding energy $B \approx -16 \text{ MeV}$, the incompressibility $K = 240 \pm 20 \text{ MeV}$,²⁸ the symmetry energy $S = 31.7 \pm 3.2 \text{ MeV}$ and its slope $L = 58.7 \pm 28.1 \text{ MeV}$.^{29,30} Combining them with the data from PREX-II,³¹ chiral effective field theory, and heavy ion collisions, more stringent constraints can be obtained.^{32,33} The observational masses and radii of PSR J0030+0451 and PSR J0740+6620,^{34–38} as well as the tidal deformability from the neutron star merger event GRB 170817A-GW170817-AT 2017gfo³⁹ will shed light on the properties of stellar matter at larger densities.

For gravity-bound stars, by combining astrophysical observations and theoretical ab initio calculations in a model-independent way, it was shown that the inferred properties of matter in the interior of most massive compact stars exhibits characteristics of the deconfined phase.¹⁰ Nevertheless, a strong first-order phase transition may be excluded due to the similarity in the radii of PSR J0030+0451 and PSR J0740+6620 despite their large differences in mass.⁴⁰ The role of strangeness in compact stars were also examined extensively,^{2–8,14–20,23,25,41–46} where additional repulsive interaction needs to be introduced to avoid the Hyperon Puzzle.²¹

Normal atomic nucleus is 2-flavoured (u and d), but “giant nucleus” at supra-nuclear densities may very well lie in the regime of 3 flavours of quarks (u , d , and s). It is thus proposed that the core-collapse compressed matter could actually be strange matter, either strange quark matter (quarks free, e.g., Refs.^{47–50}) or strangeon matter (quarks localized almost in a certain unit, called strangeon^{51,52}). The compact stars comprised of those matter are bound by strong force, which leads to a sharp decrease of density and results in a bare surface, i.e., strong-bound

stars.

In principle, a strangeon is a color singlet N_q -quark state with the number of quarks $N_q = 6, 9, 12, 15$, and 18 , which includes same amounts of u , d , and s quarks. Due to the non-observation of those multi-quark states, a strangeon may not be stable or only weakly bound in vacuum according to various investigations.^{53–61} However, if strangeons are compressed tightly together, the corresponding strangeon matter may become stable due to the strong attractive interactions,^{62–64} which could form compact stars called strangeon stars.⁶⁵ Astrophysically, observational consequences of strangeon stars show that various manifestations of pulsar-like compact objects could be interpreted in the regime of strangeon stars,^{66–73} to be tested by future advanced facilities (e.g., FAST, SKA, and eXTP). Both nuclear matter (2-flavoured) and strangeon matter (3-flavoured) can be regarded as strong condensed-matter, which is simply termed as strong matter.⁶⁵

The properties of strangeons in vacuum (i.e., H-dibaryons, strange tribaryons, etc.) were investigated extensively based on various methods. For example, their masses were obtained with QCD-inspired models, i.e., the MIT bag model,^{53–57, 74, 75} nonrelativistic quark cluster model,^{76–79} Skyrme model,^{80–83} diquark model,⁵⁸ and so on. In recent years, the properties of H-dibaryons were investigated with lattice QCD close to the physical π mass.^{59–61} However, as the number of quarks in a strangeon N_q increases, the numerical cost of lattice QCD grows drastically. Similar situation is expected for nonrelativistic quark cluster model since the number of bases grows exponentially.

The properties of strangeons in dense medium, on the other hand, are even less known. In our previous investigations, strangeons inside strangeon stars were treated as individual particles, while their interactions were taken from phenomenological potential models.^{64, 84} In this work, we attempt to obtain both the properties of strangeons and their interactions in a unified manner.

The interaction between nucleons inside nuclei was studied assuming nucleons to be bag-like. For infinite strong matter with negligible surface effect, the interactions between two or more bags can be accounted for if the bags are connected, i.e., a linked bag model, or a bag crystal model.⁸⁵ The dynamics of quark propagation between separated bags would thus introduce effective interactions so that “bags” are condensed in strong-matter. In such cases, we adopt the MIT bag model⁸⁶ to investigate the 2- and 3-flavoured strong matter in a unified manner, where quarks are assumed to be free in a bag-like hadron (perturbative QCD vacuum inside) immersed in a QCD vacuum characterized by a bag constant B . By carefully calibrate the model parameters, as will be illustrated in this work, the properties of nuclear matter, hyperon matter, and strangeon matter can be obtained simultaneously.

This paper is organized as follows. In Sec. 2, we introduce the basic framework of the linked bag model. The model is then applied to investigate the properties of nuclear matter, hyperon matter, and strangeon matter in Sec. 3, where the model parameters are fixed according to the saturation properties of nuclear matter. With the obtained equation of states (EOSs), the structures of neutron stars, hyperon

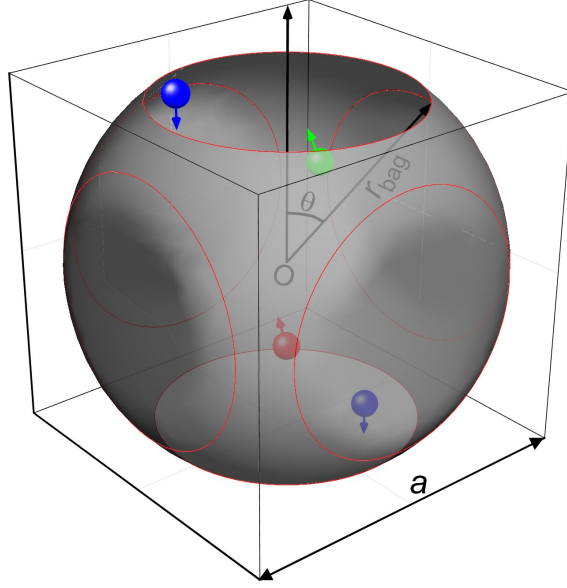


Fig. 1. A schematic illustration of a lattice cell in strong matter, in which point “O” is the center of the cell. A spherical bag (centered at “O” too) is inside the cell, which is linked to other ones through the six windows (the red circles plotted) on the bag’s surface. The size of each window is characterized by the angle θ with $\cos \theta = a/(2r_{\text{bag}})$, where a is the lattice constant and r_{bag} the bag radius.

stars, and strangeon stars are examined and confronted with astrophysical observations. We draw our conclusions in Sec. 4.

2. The linked bag model

In the linked bag model scenario, strong matter is comprised of quark bags with radius r_{bag} and quark number N_q . For simplicity, we assume that the bags arrange themselves in simple cubic lattices. The lattice constant a is related to the baryon number density n by $a = (A/n)^{1/3}$, where $A = N_q/3$ is the baryon number of a single bag in a lattice cell. If $r_{\text{bag}} > a/2$, the bags overlap with each other, and those six parts beyond the cell in Fig. 1 are cut off since they are connected with adjacent cells, leaving behind the main part of the bag with six windows on the surface. The open angle of the window is defined as $\theta = \arccos(a/2r_{\text{bag}})$. Obviously, the bag surface will disappear when $r_{\text{bag}} \geq \sqrt{3}a/2$ (i.e., $\theta \geq 54.7^\circ$), implying that strong matter may undergo a deconfinement phase transition.

Instead of solving the Dirac equations for quarks, we adopt the Fermi-gas approximation while keeping other terms from the MIT bag model. The energy per lattice cell is obtained with

$$E = \sum_j (\Omega_j + N_j \mu_j) + BV - \frac{z_0}{r_{\text{bag}}} \frac{\omega}{4\pi}, \quad (1)$$

where Ω_j , N_j and μ_j denote the thermodynamic potential, total particle number, and chemical potential of particle type j . Here after we use j for both quarks and electrons, while i only for quarks, B for the bag parameter, and V for the enclosed volume of the bag. The third term of Eq. (1) corresponds to the zero-point energy in traditional MIT bag model,⁸⁷ while here we readjust z_0 to compensate the energy shift in Fermi-gas approximations as well. The variable ω represents the solid angle of the remaining bag, which is obtained at given r_{bag} and a , i.e.,

$$\omega = \begin{cases} 4\pi, & r_{\text{bag}} < \frac{a}{2} \\ 4\pi \left(\frac{3a}{2r_{\text{bag}}} - 2 \right), & \frac{a}{2} \leq r_{\text{bag}} < \frac{\sqrt{2}a}{2} \\ \int_{\theta_1}^{\theta_2} \cos \theta \left[\frac{\pi}{2} - 2 \cos^{-1} \left(\frac{a}{2r_{\text{bag}} \cos \theta} \right) \right] d\theta, & \frac{\sqrt{2}a}{2} \leq r_{\text{bag}} < \frac{\sqrt{3}a}{2} \\ 0, & r_{\text{bag}} \geq \frac{\sqrt{3}a}{2} \end{cases}, \quad (2)$$

where $\theta_1 = \cos^{-1} \left(\frac{a}{\sqrt{2}r_{\text{bag}}} \right)$ and $\theta_2 = \sin^{-1} \left(\frac{a}{2r_{\text{bag}}} \right)$. In the extreme case of isolated bags, we have $\omega = 4\pi$ and the dimensionless parameter z_0 is fixed by fitting to hadron spectra. The solid angle ω starts to decrease from 4π when the bags are linked as indicated in Fig. 1. Once r_{bag} reaches $\sqrt{3}a/2$, ω vanishes and the bag takes up the entire volume of the lattice cell with $V = a^3$, i.e., a deconfinement phase transition that restores Eq. (1) into its original MIT bag model description of quark matter. Since we have adopted the Fermi-gas approximation instead of solving the quark single particle energies exactly, the parameter z_0 needs to vary with density to restore the discrete levels, i.e., $z_0 = z_0(n)$. In practice, we fix $z_0(n)$ by reproducing the saturation properties of nuclear matter.

The finite-size effects of the linked bag is treated with the multiple reflection expansion (MRE) method,^{88–90} where the thermodynamic potential in Eq. (1) is expanded as

$$\Omega_i = \Omega_{i,V}V + \Omega_{i,S}S + \Omega_{i,C}C. \quad (3)$$

Here the volume ($\Omega_{i,V}$), surface ($\Omega_{i,S}$), and curvature ($\Omega_{i,C}$) contributions are given by^{88–91}

$$\Omega_{i,V} = -\frac{g_i}{24\pi^2} \left[\mu_i u_i (\mu_i^2 - \frac{5}{2}m_i^2) + \frac{3}{2}m_i^4 \ln \frac{\mu_i + u_i}{m_i} \right] \quad (4)$$

$$\begin{aligned} & + \frac{g_i \alpha_s}{12\pi^3} \left[3 \left(\mu_i m_i - m_i^2 \ln \frac{\mu_i + u_i}{m_i} \right)^2 - 2u_i^4 \right. \\ & \left. + \left(6m_i^2 \ln \frac{\bar{\Lambda}}{m_i} + 4m_i^2 \right) \left(\mu_i u_i - m_i^2 \ln \frac{\mu_i + u_i}{m_i} \right) \right], \\ \Omega_{i,S} = & \frac{g_i}{8\pi} \left[\frac{\mu_i u_i^2}{6} - \frac{1}{3\pi} \left(\mu_i^3 \arctan \frac{u_i}{m_i} - 2\mu_i u_i m_i + m_i^3 \ln \frac{\mu_i + u_i}{m_i} \right) \right. \\ & \left. - \frac{m_i^2(\mu_i - m_i)}{3} \right], \end{aligned} \quad (5)$$

$$\Omega_{i,C} = \frac{g_i}{48\pi^2} \left(m_i^2 \ln \frac{\mu_i + u_i}{m_i} + \frac{\pi}{2} \frac{\mu_i^3}{m_i} - \frac{3\pi \mu_i m_i}{2} + \pi m_i^2 - \frac{\mu_i^3}{m_i} \arctan \frac{u_i}{m_i} \right), \quad (6)$$

6 *Miao, Xia, Lai, Maruyama, Xu, and Zhou*

with $u_i \equiv \sqrt{\mu_i^2 - m_i^2}$ and g_i the degeneracy factor ($g_u = g_d = g_s = 6$) for quark flavor i . The area S and curvature C of the bag are obtained with $S = \omega r_{\text{bag}}^2$ and $C = 2\omega r_{\text{bag}}$, respectively. Note that in Eq. (4) we have considered the first-order correction to the thermodynamic potential of QCD. The coupling constant α_s and quark masses m_i are running with energy scale,⁹¹ i.e.,

$$\alpha_s(\bar{\Lambda}) = \frac{1}{\beta_0 \mathfrak{L}} \left(1 - \frac{\beta_1 \ln \mathfrak{L}}{\beta_0^2 \mathfrak{L}} \right), \quad (7)$$

$$m_i(\bar{\Lambda}) = \hat{m}_i \alpha_s^{\gamma_0/\beta_0} \left[1 + \left(\frac{\gamma_1}{\beta_0} - \frac{\beta_1 \gamma_0}{\beta_0^2} \right) \alpha_s \right], \quad (8)$$

where $\mathfrak{L} = 2 \ln(\bar{\Lambda}/\Lambda_{\overline{\text{MS}}})$ and $\Lambda_{\overline{\text{MS}}}$ is the $\overline{\text{MS}}$ renormalization point. In this work we take $\Lambda_{\overline{\text{MS}}} = 376.9 \text{ MeV}$ and $\hat{m}_u = \hat{m}_d = 0$, $\hat{m}_s = 220$ and 280 MeV . The parameters of β -function and γ -function are $\beta_0 = \frac{1}{4\pi}(11 - \frac{2}{3}N_f)$, $\beta_1 = \frac{1}{16\pi^2}(102 - \frac{38}{3}N_f)$, $\gamma_0 = 1/\pi$ and $\gamma_1 = \frac{1}{16\pi^2}(\frac{202}{3} - \frac{20}{9}N_f)$ with $N_f = 3$.⁹² The renormalization scale involves with the chemical potentials of quarks, and we adopt $\bar{\Lambda} = \frac{C_1}{3} \sum_i \mu_i$ with $C_1 = 1 \sim 4$.⁹³

The bag parameter B was introduced to account for the energy difference between the physical and perturbative vacua.⁸⁶ According to QCD sum-rule,⁹⁴ one finds $B \simeq 455 \text{ MeV/fm}^3$ at vanishing chemical potentials, while fitting to the hadron spectra gives a lower value $B \simeq 50 \text{ MeV/fm}^3$.⁸⁷ At larger chemical potentials, however, it is found that B prefers a larger value by comparing with the pQCD calculations to higher orders.⁹³ To account for these values in our current study, we assume B varies with chemical potential and take a third-order expansion with respect to ξ , i.e.,

$$B = B_0 + B_2 \xi^2 + B_3 \xi^3, \quad (9)$$

where $\xi = (\sum_i N_i \mu_i / A - m_N) / m_N$ with $A (= \sum_i N_i / 3)$ being the baryon number of each lattice cell and $m_N = 938 \text{ MeV}$ the nucleon mass. This expansion is composed by three parts: the constant part B_0 , the symmetric part $B_2 \xi^2$ and the asymmetric part $B_3 \xi^3$. Note that the first-order term is discarded so that $\partial B / \partial \mu_i = 0$ at $\xi = 0$. The nuclear symmetry energy are then accounted for by taking such a form for B , since the contribution from perturbative interaction and kinetic energy of quarks does reach the experimental value of symmetry energy if we take $B_2 = B_3 = 0$. In this work we fix $B = B_0 = 50 \text{ MeV/fm}^3$ at $\sum_i N_i \mu_i / A = m_N$ ($\xi = 0$). The remaining parameters B_2 and B_3 are left undetermined and will be fixed later. The particle number N_j is then related to the chemical potentials μ_j via

$$N_j = -\frac{\partial \Omega_j}{\partial \mu_j} - \frac{\partial B}{\partial \mu_j} V. \quad (10)$$

The bag radius r_{bag} is then fixed by minimizing the total energy E at given cell volume a^3 and particle numbers N_i . With the energy per baryon determined by E/A , the energy density reads

$$\varepsilon = nE/A. \quad (11)$$

According to the basic thermodynamic relations, the baryon chemical potential and pressure are obtained with

$$\mu_b = \frac{d\varepsilon}{dn}, \quad (12)$$

$$P = n^2 \frac{d\varepsilon}{dn} = n\mu_b - \varepsilon. \quad (13)$$

3. Strong matter and compact stars

3.1. Model parameters

In our current study, the energy per baryon of both symmetric nuclear matter and neutron matter is obtained by taking $N_u = N_d = 3/2$ and $N_u = N_d/2 = 1$, respectively. At given B_2 and B_3 , the model parameters C_1 and $z_0(n_0)$ are fixed by reproducing the saturation properties of nuclear matter, while $z_0(n)$ at $n \neq n_0$ is obtained by fitting to the energy per baryon of symmetric nuclear matter. In particular, adopting the linked bag model, we reproduce the energy per baryon of nuclear matter predicted by

$$E_{\text{NM}} = E_0(n_0) + \frac{K_0}{2} \left(\frac{n - n_0}{3n_0} \right)^2 + E_{\text{sym}}(n) \delta^2 \quad (14)$$

with the symmetry energy

$$E_{\text{sym}}(n) = E_{\text{sym}}(n_0) + L \left(\frac{n - n_0}{3n_0} \right). \quad (15)$$

Here $\delta = (n_n - n_p)/n = N_d - N_u$ represents the isospin asymmetry with n_p and n_n being the proton and neutron number densities. According to various experimental investigations and nuclear theories,²⁸⁻³⁰ the parameters in Eq. (14) are well constrained. We thus take $n_0 = 0.16 \text{ fm}^{-3}$, $E_0(n_0) = 922 \text{ MeV}$, $K_0 = 240 \text{ MeV}$ and $E_{\text{sym}}(n_0) = 31.7 \text{ MeV}$, while several values of L are adopted due to its larger uncertainty.

At given B_2 and B_3 , the parameter z_0 in the linked bag model is fixed by reproducing the energy per baryon of symmetric nuclear matter obtained with Eq. (14), which is essentially density dependent and connected to the incompressibility parameter $K_0 = 240 \text{ MeV}$. Once we fix $z_0(n)$, the parameter C_1 is determined by reproducing the symmetry energy $E_{\text{sym}}(n_0) = 31.7 \text{ MeV}$. Note that the slope of symmetry energy $L(n_0)$ is essentially determined by B_2 and B_3 , so that the parameters B_2 and B_3 can be better constrained if L can be fixed. In Fig. 2 we present the constraints on the parameter set (B_2, B_3) , where we have taken either C_1 (black curves) or L (red curves) as constant values.

Based on Fig. 2, in this work we adopt four parameter sets (i-iv) with the corresponding values listed in Table 1. The obtained values of z_0 are presented in Fig. 3. It is interesting to notice that z_0 increases with density and reaches its peak value at $n \approx 3.5n_0$, which later decreases at larger densities. This may be related to the variations of nucleon structures as well as the strong correlations

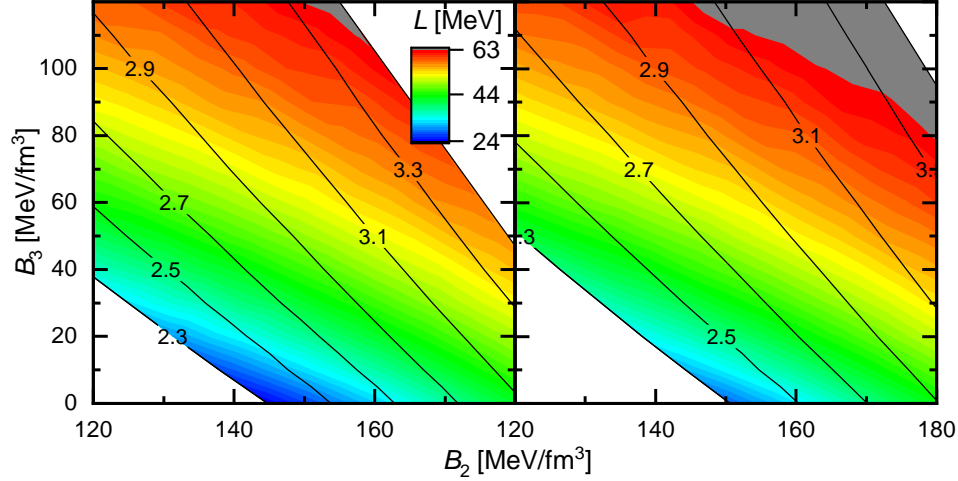


Fig. 2. The slope L of symmetry energy and B_3 obtained with various combinations of parameters B_2 , C_1 (indicated with solid curves), and two invariant strange quark masses $\hat{m}_s = 220$ MeV (Left) and 280 MeV (Right).

Table 1. Parameter sets $(C_1, \hat{m}_s, B_2, B_3, z_0(n_0))$ chosen to reproduce saturation properties of nuclear matter: the saturation density $n_0 = 0.16 \text{ fm}^{-3}$, the minimum energy per baryon $E_0(n_0) = 922$ MeV, the incompressibility $K = 240$ MeV, the symmetry energy $E_{\text{sym}}(n_0) = 31.7$ MeV. The obtained slope of symmetry energy L (in MeV) is listed here as well.

	C_1	$\hat{m}_s [\text{MeV}]$	$B_2 [\text{MeV}/\text{fm}^3]$	$B_3 [\text{MeV}/\text{fm}^3]$	$z_0(n_0)$	$L [\text{MeV}]$
(i)	2.7	220	136.7	50	2.944	45.1
(ii)	2.7	220	112.7	100	2.926	52.7
(iii)	2.7	280	125.0	100	2.908	56.6
(iv)	3.2	280	162.3	100	2.843	62.8

with neighboring nucleons in nuclear medium, e.g, the EMC effect.⁹⁵ Meanwhile, the obtained nucleon radius is decreasing with density, and approaches to a constant value at highest densities.

Since one would expect that strong interactions do not vary with quark flavor, we adopt the same values of B_0 , B_2 , and B_3 as indicated in Table 1 for hyperon and strangeon matter with $N_q \geq 3$ and $N_s \neq 0$. For the parameter z_0 , keeping it unchanged might be reasonable for $N_q = 3$. However, $z_0(n)$ could be different at larger N_q , since the quark energy level corrections should vary with respect to the quark number N_q . Note the total energy level correction takes an approximate form of $(k_1 N_q^{4/3} - k_2 N_q)/r_{\text{bag}}$, where k_1 , k_2 are two constants. To catch this feature of corrections, for simplicity, we rescale z_0 by an effective formula $z_0 = (\frac{N_q}{3})^{4/3} \tilde{z}_0 - f$, where \tilde{z}_0 is obtained by reproducing nuclear matter properties and f is a dampening

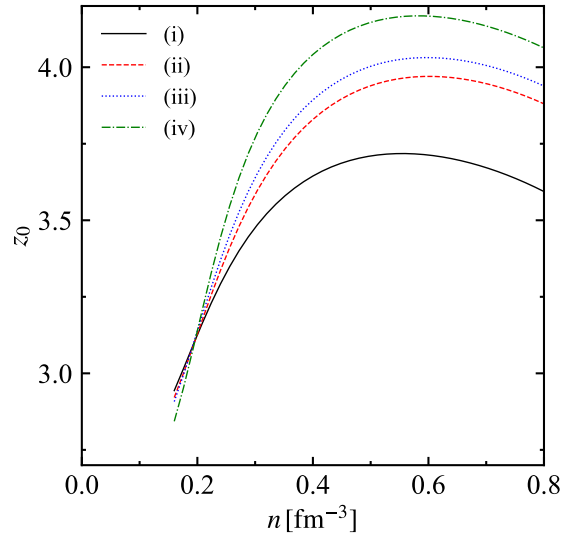


Fig. 3. The zero-point parameter as a function of baryon number density for the selected parameter sets listed in Table 1.

factor. We thus take $f = 0$ at $N_q = 3$, i.e., $z_0 = \tilde{z}_0$, while larger f is expected at larger N_q . The parameter f is then fixed by requiring the bags to be connected, which indicates $5.8 \lesssim f \lesssim 6.1$. In the discussion below, we take $f = 5.8$ since f would not significantly affect the properties of strangeon stars, as will be shown later in Sec. 3.3.

In conclusion, comparing with traditional MIT bag model,^{53–57,74,75,87} we have introduced the damping parameter f and the density dependent bag constant with two additional parameters B_2 and B_3 to account for the in-medium properties of strong matter. The possible combinations of those parameters are thoroughly examined in our current study, while the other parameters are taken as their typical values fitted to hadron spectra.⁸⁷ Note that the spin dependent interactions (e.g., the color-magnetic part of the one-gluon-exchange interaction) are not included here, which could affect the mass spectra of strangeons⁵⁵ and should be considered in our future works.

3.2. Nucleon matter, hyperon matter, and strangeon matter

In this section we study strong matter inside compact stars with linked bag model, where electrons need to be included to fulfill the charge neutrality condition

$$\sum_i Q_i N_i + Q_e N_e = 0. \quad (16)$$

Here $Q_u = 2/3$, $Q_d = Q_s = -1/3$ and $Q_e = -1$ are the charge of quarks and electrons. Note that electrons are not confined within the bags, the corresponding

thermodynamic potential can then be obtained with

$$\Omega_e = \Omega_{e,V} a^3 = -\frac{\mu_e^4}{12\pi^2} a^3. \quad (17)$$

In principle, μ^- will appear in the centre region of a neutron star. However, we neglect the contribution of μ^- since it is insignificant for hyperon stars and strangeon stars.

The quarks and leptons will undergo various weak reactions, i.e.,

$$u + e^- \rightarrow d + \nu_e, \quad d \rightarrow u + e^- + \bar{\nu}_e. \quad (18)$$

If strangeness is involved (3-flavored matter), the following reactions take place, i.e.,

$$u + e^- \rightarrow s + \nu_e, \quad s \rightarrow u + e^- + \bar{\nu}_e, \quad (19a)$$

$$s + u \leftrightarrow d + u. \quad (19b)$$

Then the β -equilibrium is reached, i.e.,

$$\mu_u + \mu_e = \mu_d = \mu_s. \quad (20)$$

In this work, the β -equilibrium condition is satisfied by minimizing the total energy with respect to the particle numbers N_i at a given total baryon number $A = \sum_i N_i/3 = N_q/3$. Then the energy density and pressure are obtained with Eqs. (11-13), which correspond to the EOS of strong matter. By taking $N_q = 3$, the EOSs of nuclear matter and hyperon matter can be obtained, while larger N_q indicates strangeon matter. In particular, we take $\hat{m}_s \rightarrow \infty$ for nuclear matter so that s quark does not emerge for β -equilibrated matter, while for hyperon matter the values indicated in Table 1 are adopted. In this paper, we limit our discussions for strong matter with $N_q = 3$ and $N_q = 9$. For all cases, as illustrated in Sec. 3.1, we keep B unchanged and $z_0 = (\frac{N_q}{3})^{4/3} \tilde{z}_0 - f$ with f being the dampening factor. Particularly, we take $f = 0$ for $N_q = 3$ and $f = 5.8$ for $N_q = 9$.

In Fig. 4 we present the energy per baryon as well as the EOSs of nuclear matter ($N_q = 3$, $N_s = 0$), hyperon matter ($N_q = 3$, $N_s \neq 0$), and strangeon matter ($N_q = 9$) in compact stars, which are obtained with the selected parameter sets in Table 1. In this work, our model is restricted to describe strong matter at $n \geq 0.16 \text{ fm}^{-3}$. In the density regime of $n < 0.16 \text{ fm}^{-3}$, we employ the results of Negele & Vautherin⁹⁶ for $0.001 \text{ fm}^{-3} < n < 0.08 \text{ fm}^{-3}$, and of Baym et al.⁹⁷ for $n < 0.001 \text{ fm}^{-3}$. Between 0.08 fm^{-3} and 0.16 fm^{-3} , we simply take a linear interpolation since the structures of neutron/hyperon stars are insensitive to the EOSs adopted in this density region. For each parameter set, the energy per baryon of nuclear matter is decreased once s -quarks (hyperons) emerge at about twice the nuclear saturation density. The energy is further reduced if we take $N_q > 3$, i.e., strangeon matter with $N_q = 9$. We note that strangeon matter reaches its minimum at $n = 2n_0 \sim 3n_0$. For a few cases, the energy per baryon of strangeon matter can even be smaller than 930 MeV, namely strangeon matter is more stable than ⁵⁶Fe.

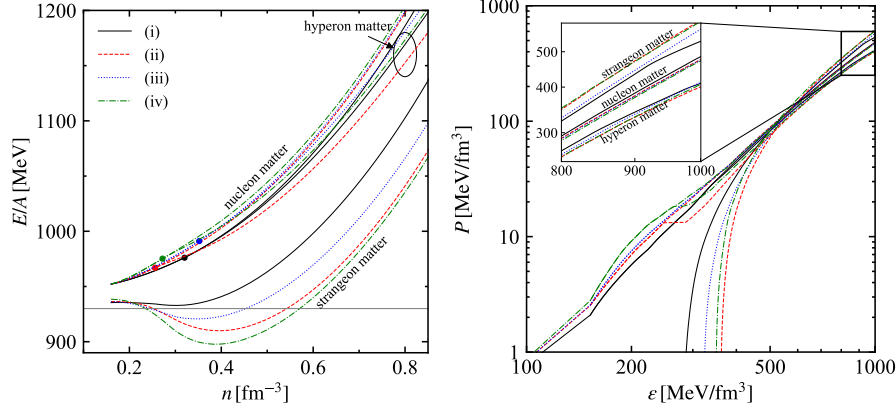


Fig. 4. Energy per baryon (Left) and the corresponding EOSs (Right) for nucleon matter with $N_q = 3$, hyperon matter with $N_q = 3$, and strangeon matter with $N_q = 9$, where the parameter sets listed in Table 1 are adopted. For strangeon matter with $N_q = 9$, we take $f = 5.8$. The horizontal line in the left panel corresponds to $E/A = 930$ MeV, which is the energy per baryon of the most stable atomic nucleus, ^{56}Fe . The solid dots indicate the critical densities at which s quark starts to appear in hyperon matter.

Table 2. The surface baryon number (n_{surf}) and energy ($\varepsilon_{\text{surf}}$) densities, radius ($R_{1.4}$), tidal deformability ($\Lambda_{1.4}$), TOV mass (M_{TOV}), and centre baryon number density (n_c) for strangeon stars obtained with the parameter sets listed in Table 1.

	$n_{\text{surf}}[\text{fm}^{-3}]$	$\varepsilon_{\text{surf}}[\text{MeV}/\text{fm}^3]$	$R_{1.4}[\text{km}]$	$\Lambda_{1.4}$	$M_{\text{TOV}}[M_\odot]$	$n_c[\text{fm}^{-3}]$
(ii)	0.395	359.38	9.519	187.9	2.411	1.069
(iii)	0.348	320.56	9.710	208.8	2.394	1.086
(iv)	0.388	348.11	9.666	210.4	2.438	1.080

Combined with Fig. 2, it is found that the minimum energy per baryon of strangeon matter increases while the corresponding density decreases along the curves with fixed C_1 from top-left to lower-right regions.

In the right panel of Fig. 4, it is easy to see that the EOSs of strangeon matter are stiffer than that of nuclear matter and hyperon matter, which indicates that the introduction of linked bag will results in stiffening of EOSs. The energy densities at zero pressure lie between ~ 280 MeV/fm³ and ~ 360 MeV/fm³, or, equivalently, ~ 1.8 and ~ 2.4 times the nuclear saturation density (mass density). It is worth noting that, although the equation of state is very stiff, the causality condition is still satisfied for strangeon matter.⁹⁸

3.3. Neutron stars, hyperon stars, and strangeon stars

The equilibrium configurations of compact stars can be obtained by solving the Tolman-Oppenheimer-Volkoff (TOV) equations for the pressure P and the enclosed

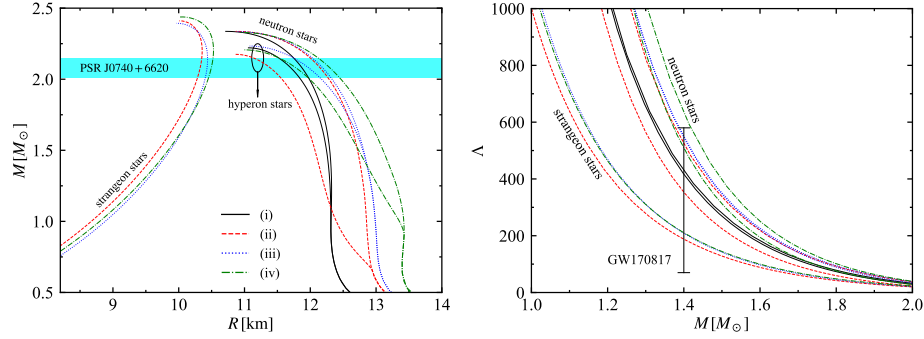


Fig. 5. Mass-radius relations (Left) and tidal deformability (Right) for traditional neutron stars, hyperon stars, and strangeon stars. For strangeon stars with $N_q = 9$, we take $f = 5.8$. The observational mass of PSR J0740+6620 ($2.08 \pm 0.07 M_\odot$)³⁸ is indicated with the horizontal band. The LIGO/Virgo constraint³⁹ from GW170817 on the tidal deformability for a $1.4 M_\odot$ star, $\Lambda_{1.4} = 190^{+390}_{-120}$, is also displayed in right panel.

mass m , i.e.,

$$\frac{dP}{dr} = -\frac{m\varepsilon}{r^2} \frac{[1 + P/\varepsilon][1 + 4\pi r^3 P/m]}{1 - 2m/r}, \quad (21)$$

$$\frac{dm}{dr} = 4\pi r^2 \varepsilon, \quad (22)$$

where P and ε are the pressure and energy density at the radial coordinate r , respectively. The dimensionless tidal deformability is related to the Love number k_2 through $\Lambda = \frac{2}{3}k_2c^{-5}$, where k_2 measures how easily a star is deformed by an external tidal field and $c = M/R$ the compactness of the star.^{99–101}

Based on the EOSs presented in Fig. 4, the mass-radius relations of compact stars are obtained by solving Eq. (21), while the tidal deformability is determined by the second Love number k_2 . The results are presented in Fig. 5, where various parameter sets listed in Table 1 are adopted. The corresponding properties of strangeon stars are listed in Table 2. In general, the maximum masses of strangeon stars are higher than those of neutron stars and hyperon stars due to the stiffer EOSs of strangeon matter. It is shown that the radius $R_{1.4}$ of a typical $1.4 M_\odot$ star ranges from 9.5 km to 13 km, where strangeon stars with $N_q = 9$ have smaller radii and larger maximum mass than those with $N_q = 3$. Note that $R_{1.4}$ generally increases with the slope of symmetry energy L for neutron stars and hyperon stars,^{32, 102–106} while such a trend is missing for strangeon stars. This is mainly due to the large surface densities ($> 2n_0$) for strangeon stars without crusts, where the saturation properties of nuclear matter have little impact on their structures. It is worth mentioning that, for strangeon stars with a smaller surface density, the radii and masses generally become larger,^{107–109} which is indeed the case for $R_{1.4}$ as indicated in Fig. 5. In the right panel of Fig. 5, we find Λ decreases monotonously with mass, while Λ is reduced with the emergence of strangeness. Except for the

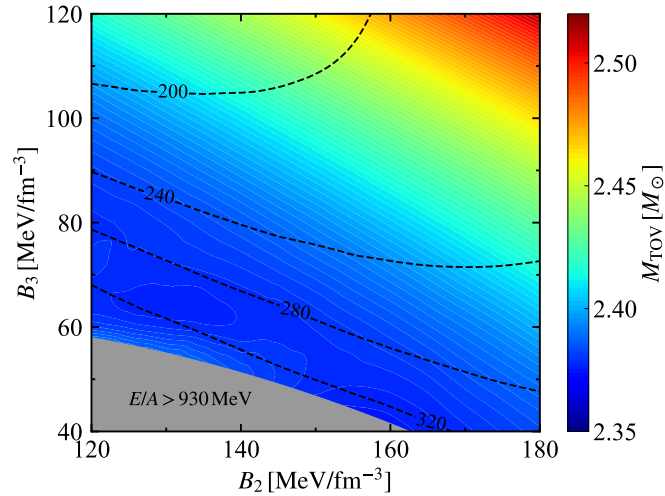


Fig. 6. Maximum mass M_{TOV} and tidal deformability of a typical $1.4 M_{\odot}$ star ($\Lambda_{1.4}$) for strangeon stars with $N_q = 9$. The invariant strange quark mass is $\hat{m}_s = 280$ MeV. Contours of M_{TOV} are illustrated in colors, while contours of $\Lambda_{1.4}$ are plotted in black dashed lines. The lower-left grey region is ruled out since strangeon matter becomes unstable with the minimum energy per baryon $E/A > 930$ MeV.

traditional neutron stars obtained with parameter set (iv), the tidal deformability of a typical $1.4 M_{\odot}$ star $\Lambda_{1.4}$ falls in between 190 and 550 for all presented cases, which fulfills the GW170817 constraint of $\Lambda_{1.4} < 580$.³⁹

To investigate the parameter dependence more carefully, in Fig. 6 we present contours of maximum mass and tidal deformability for strangeon stars. It is found that the maximum mass increases with B_2 and B_3 , which even exceeds $2.5 M_{\odot}$ in the top right corner. In light of the recent measured massive compact object (2.50 – $2.67 M_{\odot}$) in a compact binary coalescence of GW190814,¹¹⁰ the object may in fact be a strangeon star instead of a black hole. Meanwhile, even in the lower left corner, the maximum mass remains higher than $2 M_{\odot}$, which fulfills the recent observational constraints of the massive stars: PSR J1614-2230 ($1.928 \pm 0.017 M_{\odot}$),^{111,112} PSR J0740+6620 ($2.08 \pm 0.07 M_{\odot}$),³⁸ and PSR J0348+0432 ($2.01 \pm 0.04 M_{\odot}$).¹¹³ Since the central densities of $1.4 M_{\odot}$ strangeon stars are much smaller than that of the most massive ones, the tidal deformability $\Lambda_{1.4}$ is insensitive to B_2 and is decreasing slightly with B_3 . In the parameter space indicated in Fig. 6, $\Lambda_{1.4}$ ranges from 180 to 340, which fulfills the GW170817 constraint.³⁹ Note that the most recent constraints on neutron star radius by NICER³⁷ are not included in our comparison, as those analyses are based on the assumption of a normal neutron star surface instead of self-bound stars.¹¹⁴

In the discussions above, we have fixed $f = 5.8$ for strangeon stars with $N_q = 9$. However, f is a free parameter introduced to denote the energy level correction

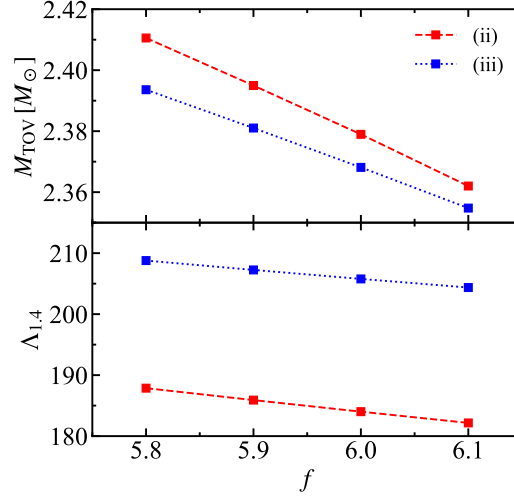


Fig. 7. Maximum mass M_{TOV} and tidal deformability ($\Lambda_{1.4}$) of strangeon stars as functions of the dampening factor f .

and the exact value of f is unknown. It is thus meaningful to investigate the effects of f on strangeon star structures. For this reason, in Fig. 7 we present the maximum mass M and tidal deformability ($\Lambda_{1.4}$) of strangeon stars as functions of the dampening factor f . In general, the maximum mass and tidal deformability monotonously decrease with f . At lower f , the maximum mass M_{TOV} may exceeds $2.4 M_{\odot}$. We also notice for both cases displayed in Fig. 7, $\Lambda_{1.4}$ lies in the range of GW170817 constraint.³⁹ In a word, there exists a large parameter space for f that the linked bag model predicts compact star structures satisfying the observational constraints on mass and tidal deformability.

4. Discussions and Conclusions

The nature of gravity-compressed baryon matter created after core-collapsed supernova is investigated in this work, where both 2-flavoured nucleon and 3-flavoured strangeon matters are modeled with linked bags. At this moment, pulsars are usually thought to be conventional neutron stars, while they could be strange quark stars if Witten's conjecture⁴⁷ is correct. Unfortunately, it is still challenging to prove or disprove this conjecture because of the non-perturbative behavior of strong interaction. 3-flavoured quarks could be grouped in strange-clusters/strangeons if the coupling between quarks is still strong enough, where a self-bound strangeon star can be formed. This speculative view of strangeon star has been supported by latter astronomical observations, particularly the discovery of massive radio pulsars around $2M_{\odot}$ ^{111–113} since the EOS of strangeon matter is very stiff.⁸⁴ A strangeon star model of pulsar glitch was proposed,^{72, 115} and the shear modulus of strangeon

matter is constrained to be order of 10^{34} erg/cm³ in order to explain the glitch activity. In addition to the glitch phenomenon, a recent hot topic of fast radio bursts could also be interesting events to reveal the magnetospheric activity of strangeon stars.^{116,117} Note that if atomic line feature would be discovered in X-ray spectrum of radio pulsars, the strangeon star model has to be ruled out.¹¹⁸ It is, therefore, urgent to model strangeon matter with microscopic foundation in consistent with nuclear physics, in order to predict effectively astronomical observations in the future. Here we try to do so with a linked-bag model, as a first step, in the regime of non-perturbative QCD.

In this paper, we model the strong condensed matter of 3-flavoured strangeons with a linked bag approach. For fixed bag parameters B_2 and B_3 , the model parameters C_1 and z_0 are calibrated by reproducing the saturation properties (E/A , K_0 , E_{sym} and L) of nucleon matter. Beside these, a dampening factor f is introduced to account for the reduction of quark energy level corrections. The obtained energy per baryon of strangeon matter is usually smaller than that of nuclear and hyperon matter, which can be further reduced if we adopt larger quark numbers (N_q) inside a strangeon. The corresponding EOSs of strangeon matter become stiffer as well, which increases the maximum mass of strangeon stars. It is found that, for $N_q = 9$, the maximum mass of strangeon stars could be $\sim 2.5M_\odot$, while the tidal deformability of a $1.4M_\odot$ strangeon star $\Lambda_{1.4} \simeq (180-340)$. To investigate the parameter dependence, the maximum mass and tidal deformability of strangeon stars predicted by the linked bag model are examined by adopting various B_2 , B_3 , and f , which are consistent with the current astrophysical constraints in a large parameter space. More refined theoretical efforts are required in our future study, where the quark single particle energy,⁸⁵ the interactions among quarks (instanton, electric and magnetic gluon exchange, etc.), the center-of-mass correction,¹¹⁹ the effects of color superconductivity,^{120,121} the quark composition of strangeons, and the possible mixing of different types of strangeons and baryons should be examined carefully. Those effects could easily alter our predictions on M_{TOV} and $\Lambda_{1.4}$ of strangeon stars, which should be tested further in the era of multi-messenger astronomy.

ACKNOWLEDGMENTS

We would like to thank Prof. Guangshan Tian for discussion relevant to normal condensed matter, Prof. Ang Li and Prof. Makoto Oka for valuable comments and suggestions, and Mr. Yong Gao and Dr. Fei He for a preliminary calculation. This work was supported by National SKA Program of China No. 2020SKA0120300, National Key R&D Program of China (Grant No. 2017YFA0402602), the National Natural Science Foundation of China (Grant Nos. 11673002, U1531243, U1831104).

References

1. A. Li, Z.-Y. Zhu, E.-P. Zhou, J.-M. Dong, J.-N. Hu and C.-J. Xia, *JHEAP* **28** (2020) 19.
2. S. Weissenborn, I. Sagert, G. Pagliara, M. Hempel and J. Schaffner-Bielich, *Astrophys. J.* **740** (2011) L14.
3. T. Klähn, R. Lastowiecki and D. Blaschke, *Phys. Rev. D* **88** (Oct 2013) 085001.
4. T. Zhao, S.-S. Xu, Y. Yan, X.-L. Luo, X.-J. Liu and H.-S. Zong, *Phys. Rev. D* **92** (Sep 2015) 054012.
5. T. Kojo, P. D. Powell, Y. Song and G. Baym, *Phys. Rev. D* **91** (Feb 2015) 045003.
6. A. Li, W. Zuo and G. X. Peng, *Phys. Rev. C* **91** (Mar 2015) 035803.
7. K. Masuda, T. Hatsuda and T. Takatsuka, *Eur. Phys. J. A* **52** (2016) 65.
8. D. L. Whittenbury, H. H. Matevosyan and A. W. Thomas, *Phys. Rev. C* **93** (Mar 2016) 035807.
9. N.-U. F. Bastian, D. Blaschke, T. Fischer and G. Röpke, *Universe* **4** (2018) 67.
10. E. Annala, T. Gorda, A. Kurkela, J. Nättilä and A. Vuorinen, *Nat. Phys.* **16** (2020) 907.
11. D. Blaschke, A. Ayriyan, D. E. Alvarez-Castillo and H. Grigorian, *Universe* **6** (2020) 81.
12. D. Blaschke and D. Alvarez-Castillo, *Eur. Phys. J. A* **56** (2020) 124.
13. C.-J. Xia, T. Maruyama, N. Yasutake, T. Tatsumi, H. Shen and H. Togashi, *Phys. Rev. D* **102** (Jul 2020) 023031.
14. S. Weissenborn, D. Chatterjee and J. Schaffner-Bielich, *Phys. Rev. C* **85** (Jun 2012) 065802.
15. Bednarek, I., Haensel, P., Zdunik, J. L., Bejger, M. and Mařka, R., *Astron. Astrophys.* **543** (2012) A157.
16. M. Oertel, C. Providência, F. Gulminelli and A. R. Raduta, *J. Phys. G: Nucl. Part. Phys.* **42** (2015) 075202.
17. K. Maslov, E. Kolomeitsev and D. Voskresensky, *Nucl. Phys. A* **950** (2016) 64 .
18. T. Takatsuka, S. Nishizaki and Y. Yamamoto, *Eur. Phys. J. A* **13** (2002) 213.
19. D. Lonardoni, A. Lovato, S. Gandolfi and F. Pederiva, *Phys. Rev. Lett.* **114** (Mar 2015) 092301.
20. H. Togashi, E. Hiyama, Y. Yamamoto and M. Takano, *Phys. Rev. C* **93** (Mar 2016) 035808.
21. I. Vidaña, *AIP Conf. Proc.* **1645** (2015) 79.
22. M. Fortin, S. S. Avancini, C. Providência and I. Vidaña, *Phys. Rev. C* **95** (Jun 2017) 065803.
23. T.-T. Sun, C.-J. Xia, S.-S. Zhang and M. S. Smith, *Chin. Phys. C* **42** (2018) 025101.
24. B. Holdom, J. Ren and C. Zhang, *Phys. Rev. Lett.* **120** (May 2018) 222001.
25. T.-T. Sun, S.-S. Zhang, Q.-L. Zhang and C.-J. Xia, *Phys. Rev. D* **99** (Jan 2019) 023004.
26. T. Zhao, W. Zheng, F. Wang, C.-M. Li, Y. Yan, Y.-F. Huang and H.-S. Zong, *Phys. Rev. D* **100** (Aug 2019) 043018.
27. C. Zhang, *Phys. Rev. D* **101** (Feb 2020) 043003.
28. S. Shlomo, V. M. Kolomietz and G. Colò, *Eur. Phys. J. A* **30** (Oct 2006) 23.
29. B.-A. Li and X. Han, *Phys. Lett. B* **727** (2013) 276 .
30. M. Oertel, M. Hempel, T. Klähn and S. Typel, *Rev. Mod. Phys.* **89** (Mar 2017) 015007.
31. PREX Collaboration, *Phys. Rev. Lett.* **126** (Apr 2021) 172502.
32. Y. Zhang, M. Liu, C.-J. Xia, Z. Li and S. K. Biswal, *Phys. Rev. C* **101** (Mar 2020) 034303.

33. R. Essick, I. Tews, P. Landry and A. Schwenk, *Phys. Rev. Lett.* **127** (Nov 2021) 192701.
34. T. E. Riley, A. L. Watts, S. Bogdanov, P. S. Ray, R. M. Ludlam, S. Guillot, Z. Arzoumanian, C. L. Baker, A. V. Bilous, D. Chakrabarty, K. C. Gendreau, A. K. Harding, W. C. G. Ho, J. M. Lattimer, S. M. Morsink and T. E. Strohmayer, *Astrophys. J.* **887** (Dec 2019) L21.
35. T. E. Riley, A. L. Watts, P. S. Ray, S. Bogdanov, S. Guillot, S. M. Morsink, A. V. Bilous, Z. Arzoumanian, D. Choudhury, J. S. Deneva, K. C. Gendreau, A. K. Harding, W. C. G. Ho, J. M. Lattimer, M. Loewenstein, R. M. Ludlam, C. B. Markwardt, T. Okajima, C. Prescod-Weinstein, R. A. Remillard, M. T. Wolff, E. Fonseca, H. T. Cromartie, M. Kerr, T. T. Pennucci, A. Parthasarathy, S. Ransom, I. Stairs, L. Guillemot and I. Cognard, *Astrophys. J.* **918** (Sep 2021) L27.
36. M. C. Miller, F. K. Lamb, A. J. Dittmann, S. Bogdanov, Z. Arzoumanian, K. C. Gendreau, S. Guillot, A. K. Harding, W. C. G. Ho, J. M. Lattimer, R. M. Ludlam, S. Mahmoodifar, S. M. Morsink, P. S. Ray, T. E. Strohmayer, K. S. Wood, T. Enoto, R. Foster, T. Okajima, G. Prigozhin and Y. Soong, *Astrophys. J.* **887** (Dec 2019) L24.
37. M. C. Miller, F. K. Lamb, A. J. Dittmann, S. Bogdanov, Z. Arzoumanian, K. C. Gendreau, S. Guillot, W. C. G. Ho, J. M. Lattimer, M. Loewenstein, S. M. Morsink, P. S. Ray, M. T. Wolff, C. L. Baker, T. Cazeau, S. Manthripragada, C. B. Markwardt, T. Okajima, S. Pollard, I. Cognard, H. T. Cromartie, E. Fonseca, L. Guillemot, M. Kerr, A. Parthasarathy, T. T. Pennucci, S. Ransom and I. Stairs, *Astrophys. J.* **918** (Sep 2021) L28.
38. E. Fonseca, H. T. Cromartie, T. T. Pennucci, P. S. Ray, A. Y. Kirichenko, S. M. Ransom, P. B. Demorest, I. H. Stairs, Z. Arzoumanian, L. Guillemot, A. Parthasarathy, M. Kerr, I. Cognard, P. T. Baker, H. Blumer, P. R. Brook, M. DeCesar, T. Dolch, F. A. Dong, E. C. Ferrara, W. Fiore, N. Garver-Daniels, D. C. Good, R. Jennings, M. L. Jones, V. M. Kaspi, M. T. Lam, D. R. Lorimer, J. Luo, A. McEwen, J. W. McKee, M. A. McLaughlin, N. McMann, B. W. Meyers, A. Naidu, C. Ng, D. J. Nice, N. Pol, H. A. Radovan, B. Shapiro-Albert, C. M. Tan, S. P. Tendulkar, J. K. Swiggum, H. M. Wahl and W. W. Zhu, *Astrophys. J.* **915** (Jul 2021) L12.
39. LIGO Scientific and Virgo Collaborations, *Phys. Rev. Lett.* **121** (2018) 161101.
40. P. T. H. Pang, I. Tews, M. W. Coughlin, M. Bulla, C. V. D. Broeck and T. Dietrich, *Astrophys. J.* **922** (Nov 2021) 14.
41. K. Maslov, E. Kolomeitsev and D. Voskresensky, *Phys. Lett. B* **748** (2015) 369 .
42. I. Vidaña, D. Logoteta, C. Providência, A. Polls and I. Bombaci, *Europhys. Lett.* **94** (2011) 11002.
43. Y. Yamamoto, T. Furumoto, N. Yasutake and T. A. Rijken, *Phys. Rev. C* **88** (Aug 2013) 022801.
44. K. Fukushima and T. Kojo, *Astrophys. J.* **817** (2016) 180.
45. V. Dexheimer, R. O. Gomes, T. Klähn, S. Han and M. Salinas, *Phys. Rev. C* **103** (Feb 2021) 025808.
46. Z.-H. Tu and S.-G. Zhou, *Astrophys. J.* **925** (Jan 2022) 16.
47. E. Witten, *Phys. Rev. D* **30** (Jul 1984) 272.
48. P. Haensel, J. L. Zdunik and R. Schaeffer., *Astron. Astrophys.* **160** (1986) 121.
49. C. Alcock, E. Farhi and A. Olinto, *Astrophys. J.* **310** (Nov 1986) 261.
50. F. Weber, *Prog. Part. Nucl. Phys.* **54** (2005) 193.
51. R.-X. Xu, *Astrophys. J.* **596** (2003) L59.
52. W. Wang, J. Lu, H. Tong, M. Ge, Z. Li, Y. Men and R. Xu, *Astrophys. J.* **837** (Mar 2017) 81.

18 Miao, Xia, Lai, Maruyama, Xu, and Zhou

53. R. L. Jaffe, *Phys. Rev. Lett.* **38** (Jan 1977) 195.
54. R. L. Jaffe, *Phys. Rev. Lett.* **38** (Mar 1977) 617.
55. A. T. M. Aerts, P. J. G. Mulders and J. J. de Swart, *Phys. Rev. D* **17** (Jan 1978) 260.
56. K. Maltman, *Phys. Lett. B* **291** (1992) 371 .
57. Y. Maezawa, T. Hatsuda and S. Sasaki, *Prog. Theor. Phys.* **114** (2005) 317.
58. S. H. Lee and S. Yasui, *Eur. Phys. J. C* **64** (2009) 283.
59. NPLQCD Collaboration Collaboration (S. R. Beane, E. Chang, W. Detmold, B. Joo, H. W. Lin, T. C. Luu, K. Orginos, A. Parreño, M. J. Savage, A. Torok and A. Walker-Loud), *Phys. Rev. Lett.* **106** (Apr 2011) 162001.
60. HAL QCD Collaboration Collaboration (T. Inoue, N. Ishii, S. Aoki, T. Doi, T. Hatsuda, Y. Ikeda, K. Murano, H. Nemura and K. Sasaki), *Phys. Rev. Lett.* **106** (Apr 2011) 162002.
61. K. Sasaki, S. Aoki, T. Doi, S. Gongyo, T. Hatsuda, Y. Ikeda, T. Inoue, T. Iritani, N. Ishii, K. Murano and T. Miyamoto, *Nucl. Phys. A* **998** (2020) 121737.
62. T. Sakai, J. Mori, A. Buchmann, K. Shimizu and K. Yazaki, *Nucl. Phys. A* **625** (1997) 192 .
63. N. K. Glendenning and J. Schaffner-Bielich, *Phys. Rev. C* **58** (Aug 1998) 1298.
64. X. Y. Lai, C. Y. Gao and R. X. Xu, *Mon. Not. R. Astron. Soc.* **431** (2013) 3282.
65. R. Xu, *Sci. China-Phys. Mech. Astron.* **61** (May 2018) 109531.
66. J. E. Horvath, *Mod. Phys. Lett. A* **20** (2005) 2799.
67. B. J. Owen, *Phys. Rev. Lett.* **95** (Nov 2005) 211101.
68. M. Mannarelli, K. Rajagopal and R. Sharma, *Phys. Rev. D* **76** (Oct 2007) 074026.
69. X. Lai and R. Xu, *J. Phys: Conf. Ser.* **861** (Jun 2017) 012027.
70. X. Lai, E. Zhou and R. Xu, *Eur. Phys. J. A* **55** (Apr 2019) 60.
71. X.-Y. Lai, C.-J. Xia, Y.-W. Yu and R.-X. Xu, *Res. Astron. Astrophys.* **21** (Nov 2021) 250.
72. W. H. Wang, X. Y. Lai, E. P. Zhou, J. G. Lu, X. P. Zheng and R. X. Xu, *Mon. Not. R. Astron. Soc.* **500** (Nov 2021) 5336.
73. Y. Gao, X.-Y. Lai, L. Shao and R.-X. Xu, *Mon. Not. R. Astron. Soc.* **509** (Nov 2021) 2758.
74. P. J. Mulders, A. T. Aerts and J. J. de Swart, *Phys. Rev. D* **21** (May 1980) 2653.
75. K. Liu and C. Wong, *Phys. Lett. B* **113** (1982) 1 .
76. M. Oka, K. Shimizu and K. Yazaki, *Phys. Lett. B* **130** (1983) 365.
77. U. Straub, Z.-Y. Zhang, K. Brauer, A. Faessler and S. Khadkikar, *Phys. Lett. B* **200** (1988) 241.
78. M. Oka and S. Takeuchi, *Nucl. Phys. A* **524** (1991) 649.
79. P. Shen, Z. Zhang, Y. Yu, X. Yuan and S. Yang, *J. Phys. G* **25** (1999) 1807.
80. A. P. Balachandran, A. Barducci, F. Lizzi, V. G. J. Rodgers and A. Stern, *Phys. Rev. Lett.* **52** (Mar 1984) 887.
81. R. Jaffe and C. Korpa, *Nucl. Phys. B* **258** (1985) 468.
82. S. A. Yost and C. R. Nappi, *Phys. Rev. D* **32** (1985) 816.
83. V. Kopeliovich, B. Schwesinger and B. Stern, *Nucl. Phys. A* **549** (1992) 485.
84. X. Y. Lai and R. X. Xu, *Mon. Not. Roy. Astron. Soc.* **398** (09 2009) L31.
85. Q.-R. Zhang and H.-M. Liu, *Phys. Rev. C* **46** (Dec 1992) 2294.
86. A. Chodos, R. L. Jaffe, K. Johnson, C. B. Thorn and V. F. Weisskopf, *Phys. Rev. D* **9** (Jun 1974) 3471.
87. T. DeGrand, R. L. Jaffe, K. Johnson and J. Kiskis, *Phys. Rev. D* **12** (Oct 1975) 2060.
88. M. S. Berger and R. L. Jaffe, *Phys. Rev. C* **35** (Jan 1987) 213.

89. M. S. Berger and R. L. Jaffe, *Phys. Rev. C* **44** (Jul 1991) 566.
90. J. Madsen, *Phys. Rev. D* **50** (Sep 1994) 3328.
91. E. S. Fraga and P. Romatschke, *Phys. Rev. D* **71** (May 2005) 105014.
92. J. Vermaseren, S. Larin and T. van Ritbergen, *Phys. Lett. B* **405** (1997) 327 .
93. E. S. Fraga, A. Kurkela and A. Vuorinen, *Astrophys. J.* **781** (2014) L25.
94. E. Shuryak, *Phys. Lett. B* **79** (1978) 135.
95. European Muon Collaboration, *Phys. Lett. B* **123** (1983) 275 .
96. J. W. Negele and D. Vautherin, *Nucl. Phys. A* **207** (June 1973) 298.
97. G. Baym, C. Pethick and P. Sutherland, *Astrophys. J.* **170** (December 1971) 299.
98. J. Lu, E. Zhou, X. Lai and R. Xu, *Sci. China Phys. Mech. Astron.* **61** (2018) 089511.
99. T. Damour and A. Nagar, *Phys. Rev. D* **80** (Oct 2009) 084035.
100. T. Hinderer, B. D. Lackey, R. N. Lang and J. S. Read, *Phys. Rev. D* **81** (Jun 2010) 123016.
101. S. Postnikov, M. Prakash and J. M. Lattimer, *Phys. Rev. D* **82** (Jul 2010) 024016.
102. Z.-Y. Zhu, E.-P. Zhou and A. Li, *Astrophys. J.* **862** (2018) 98.
103. M. Tsang, W. Lynch, P. Danielewicz and C. Tsang, *Phys. Lett. B* **795** (2019) 533 .
104. V. Dexheimer, R. de Oliveira Gomes, S. Schramm and H. Pais, *J. Phys. G: Nucl. Part. Phys.* **46** (Feb 2019) 034002.
105. N.-B. Zhang and B.-A. Li, *Eur. Phys. J. A* **55** (2019) 39.
106. B.-A. Li and M. Magno, *Phys. Rev. C* **102** (Oct 2020) 045807.
107. S. Bhattacharyya, I. Bombaci, D. Logoteta and A. V. Thampan, *Mon. Not. R. Astron. Soc.* **457** (Jan 2016) 3101.
108. A. Li, Z.-Y. Zhu and X. Zhou, *Astrophys. J.* **844** (Jul 2017) 41.
109. C.-J. Xia, Z. Zhu, X. Zhou and A. Li, *Chin. Phys. C* **45** (2021) 055104.
110. LIGO Scientific and Virgo Collaborations, *Astrophys. J.* **896** (Jun 2020) L44.
111. P. B. Demorest, T. Pennucci, S. M. Ransom, M. S. E. Roberts and J. W. T. Hessels, *Nature* **467** (2010) 1081.
112. E. Fonseca, T. T. Pennucci, J. A. Ellis, I. H. Stairs, D. J. Nice, S. M. Ransom, P. B. Demorest, Z. Arzoumanian, K. Crowter, T. Dolch, R. D. Ferdman, M. E. Gonzalez, G. Jones, M. L. Jones, M. T. Lam, L. Levin, M. A. McLaughlin, K. Stovall, J. K. Swiggum and W. Zhu, *Astrophys. J.* **832** (2016) 167.
113. J. Antoniadis, P. C. C. Freire, N. Wex, T. M. Tauris, R. S. Lynch, M. H. van Kerkwijk, M. Kramer, C. Bassa, V. S. Dhillon, T. Driebe, J. W. T. Hessels, V. M. Kaspi, V. I. Kondratiev, N. Langer, T. R. Marsh, M. A. McLaughlin, T. T. Pennucci, S. M. Ransom, I. H. Stairs, J. van Leeuwen, J. P. W. Verbiest and D. G. Whelan, *Science* **340** (2013) 1233232.
114. A. Li, Z.-Q. Miao, J.-L. Jiang, S.-P. Tang and R.-X. Xu, *Mon. Not. R. Astron. Soc.* **506** (Jul 2021) 5916.
115. X. Y. Lai, C. A. Yun, J. G. Lu, G. L. Lü, Z. J. Wang and R. X. Xu, *Mon. Not. R. Astron. Soc.* **476** (Feb 2018) 3303.
116. W. Wang, R. Luo, H. Yue, X. Chen, K. Lee and R. Xu, *Astrophys. J.* **852** (Jan 2018) 140.
117. R. Luo, B. J. Wang, Y. P. Men, C. F. Zhang, J. C. Jiang, W. Y. L. K. J. H. J. L. Z. B. C. R. N. C. M. Z. Xu, H. and Wang, X. L. Chen, H. Q. Gan, Y. J. Guo, L. F. Hao, Y. X. Huang, P. Jiang, H. Li, J. Li, Z. X. Li, J. T. Luo, J. Pan, X. Pei, L. Qian, J. H. Sun, M. Wang, N. Wang, Z. G. Wen, R. X. Xu, Y. H. Xu, J. Yan, W. M. Yan, D. J. Yu, J. P. Yuan, S. B. Zhang and Y. Zhu, *Nature* **586** (Oct 2020) 693.
118. R. X. Xu, G. J. Qiao and B. Zhang, *Astrophys. J.* **522** (Sep 1999) L109.
119. J. Bartelski, A. Szymacha, L. Mankiewicz and S. Tatur, *Phys. Rev. D* **29** (Mar 1984) 1035.

20 *Miao, Xia, Lai, Maruyama, Xu, and Zhou*

120. M. Buballa, *Phys. Rep.* **407** (2005) 205.

121. M. G. Alford, A. Schmitt, K. Rajagopal and T. Schäfer, *Rev. Mod. Phys.* **80** (Nov 2008) 1455.